Structure-Based Design Guides the Improved Efficacy of Deacylation Transition State Analogue Inhibitors of TEM-1 β-Lactamase[†,#]

Steven Ness,[‡] Richard Martin,[§] Alois M. Kindler,[§] Mark Paetzel,[‡] Marvin Gold,[||] Susan E. Jensen,[⊥] J. Bryan Jones,[§] and Natalie C. J. Strynadka*[,‡]

Department of Biochemistry and Molecular Biology, University of British Columbia, 2146 Health Sciences Mall, Vancouver, British Columbia, Canada, V6T 1Z3, Departments of Chemistry and of Molecular and Medical Genetics, University of Toronto, 80 St. George Street, Toronto, Ontario, Canada, M5S 1A1, and Department of Biological Sciences, University of Alberta, Edmonton, Alberta, Canada, T6G 2H7

Received October 28, 1999; Revised Manuscript Received January 31, 2000

ABSTRACT: Transition state analogue boronic acid inhibitors mimicking the structures and interactions of good penicillin substrates for the TEM-1 β-lactamase of *Escherchia coli* were designed using graphic analyses based on the enzyme's 1.7 Å crystallographic structure. The synthesis of two of these transition state analogues, (1*R*)-1-phenylacetamido-2-(3-carboxyphenyl)ethylboronic acid (**1**) and (1*R*)-1-acetamido-2-(3-carboxy-2-hydroxyphenyl)ethylboronic acid (**2**), is reported. Kinetic measurements show that, as designed, compounds **1** and **2** are highly effective deacylation transition state analogue inhibitors of TEM-1 β-lactamase, with inhibition constants of 5.9 and 13 nM, respectively. These values identify them as among the most potent competitive inhibitors yet reported for a β-lactamase. The best inhibitor of the current series was (1*R*)-1-phenylacetamido-2-(3-carboxyphenyl)ethylboronic acid (**1**, $K_I = 5.9$ nM), which resembles most closely the best known substrate of TEM-1, benzylpenicillin (penicillin G). The high-resolution crystallographic structures of these two inhibitors covalently bound to TEM-1 are also described. In addition to verifying the design features, these two structures show interesting and unanticipated changes in the active site area, including strong hydrogen bond formation, water displacement, and rearrangement of side chains. The structures provide new insights into the further design of this potent class of β-lactamase inhibitors.

β-Lactamases are the major cause of antibiotic resistance to the family of β-lactam antibiotics including the widely administered penicillins and cephalosporins (*1*−*4*). These bacterial enzymes catalyze the demise of these antibiotics through an incredibly efficient hydrolysis of the lactam bond. TEM-1 is a representative member of the group 2b (*5*) or class A β-lactamases that has achieved particular clinical notoriety: its plasmid-encoded nature coupled with a rapidly increasing number of site-specific mutations have led to a whole family of TEM enzymes which are resistant to an increasing spectrum of β-lactam antibiotics (*6*). The design and synthesis of β-lactamase inhibitors represents one strategy for combating the β-lactam deactivating capacities of these enzymes. Clinically, the most widely used β-lactamase inhibitors are β-lactams themselves [clavulanic acid and tazobactam are prominent examples (*7, 8*)]. With bacterial resistance to these inhibitors continuing to increase, especially among the TEM enzymes, identification of new structural classes of β-lactamase inhibitors is of utmost clinical importance. To this end, there have recently been several elegant studies using a variety of approaches for the design of novel mechanism-based class A β-lactamase inhibitors including phosphonate derivatives (*9*−*13*), sulfone derivatives (*14, 15*), and substrate analogues (*16*−*18*).

The 1.7 Å resolution X-ray structure of class A TEM-1 β-lactamase from *E. coli* covalently bound to a penicillin G substrate has been reported (*19*). These data, and the mechanistic insights they revealed, prompted us to take an alternative approach to β-lactamase inhibitor design by utilizing boronic acids as potential inhibitors for this enzyme. Boronic acid was particularly attractive in this regard since it had been previously shown by ^{11}B NMR spectroscopy to be a reversible transition state analogue inhibitor that forms tetrahedral adducts with the active site serine of β-lactamases (*20*). Very recently, derivatives of boronic acids have also shown to be excellent inhibitors of the class C β-lactamases (*21*). Building on the X-ray data, and our previous experience in boronic acid inhibition of this enzyme (*22*−*24*), we have identified structures with the potential to be highly effective transition state analogue inhibitors. In this rational design process, the active site interactions of representative penicillin substrates (Figure 1a) were first identified. Using molecular

[†] We thank the Natural Sciences and Engineering Research Council of Canada for support (to J.B.J., S.E.J., and N.C.J.S.), the University of Toronto for an Open Doctoral Fellowship (to R.M.), the Deutsche Forschung Gemeinschaft for a postdoctoral fellowship (to A.M.K.), the Medical Research Council of Canada for a grant (to N.C.J.S.), and Dr. Malcolm Capel for use of NSLS beamline X12B.

[#] Coordinates have been deposited in the Protein Data Bank under numbers 1ERM, 1ERO, and 1ERQ.

* To whom correspondence should be addressed at the University of British Columbia, Department of Biochemistry and Molecular Biology, Faculty of Medicine, 2146 Health Sciences Mall, Vancouver, BC, Canada V6T 1Z3. Tel.: 604-822-8032 (lab) or 604-822-0789 (office), Fax: 604-822-5227, email: natalie@byron.biochem.ubc.ca.

[‡] Department of Biochemistry and Molecular Biology, Univiersity of British Columbia.

[§] Department of Chemistry, University of Toronto.

[||] Department of Molecular and Medical Genetics, University of Toronto.

[⊥] Department of Biological Sciences, University of Alberta.

10.1021/bi992505b CCC: $19.00
Published on Web 04/15/2000

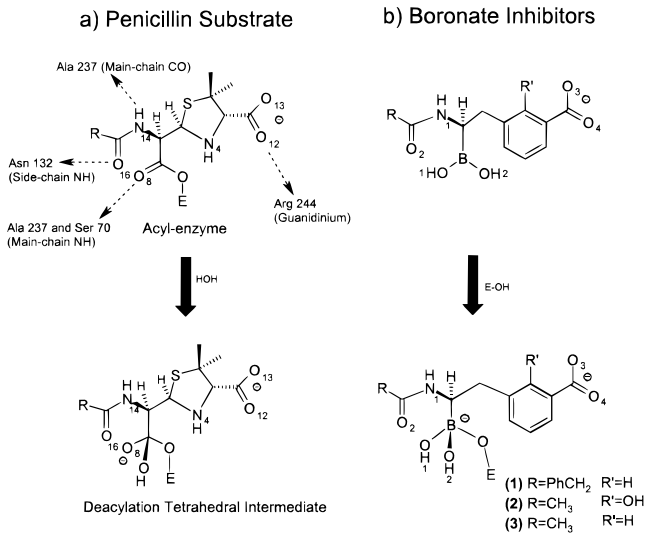

FIGURE 1: (a) Schematic of the experimentally determined acyl-enzyme complex (*19*) showing the active site interactions considered to play a key role in the binding of the TEM1 β-lactamase with penicillin G, and upon which the designs of the transition state analogue inhibitors were based. (b) Boronic acid deacylation transition state analogue inhibitors designed to mimic the binding patterns depicted in (a). The variations of compounds **1** and **2** (presented in this paper) and the initially designed *N*-acetyl derivative (compound **3**; *22*−*24*) are depicted as R and R′ in the diagram.

modeling, variants of boronic acids containing the appropriate chemical adducts were constructed which would best mimic the critical interactions observed in the penicillin G/TEM-1 complex (Figure 1b). The key features of the design are as follows: (i) interaction of the electrophilic boron with the active site Ser 70 to form a tetrahedral intermediate such that the boronate center would be stabilized within the oxyanion hole of the enzyme (the two main chain nitrogen atoms of Ala 237 and Ser 70); (ii) correct orientation of the phenylacetyl side chain to elicit the desired hydrogen-bonding interactions with the main chain carbonyl oxygen of Ala 237 and the side chain amide nitrogen of Asn 132; (iii) suitable positioning of the inhibitor carboxylate moiety for electrostatic and hydrogen-bonding interactions with the conserved residues Lys 234, Ser 235, and Arg 244. The first of these compounds to be synthesized, (1*R*)-1-acetamido-2-(3-carboxyphenyl)ethaneboronic acid (compound **3** in Figure 1), showed excellent inhibition properties (K_i = 110 nM), giving credence to our design efforts (*22*−*24*). The results presented here build on this previous work through the structure-guided incorporation of additional side chain functionalities (compound **1**) or hydrogen bonding groups (compound **2**) to maximize energetically favorable interactions of the boronate inhibitors and TEM-1 β-lactamase.

The side chain phenylacetamido moiety of **1** was chosen as it is present in penicillin G, itself an excellent substrate of class A β-lactamases. The 1.7 Å resolution structure of penicillin G bound as an acyl-enzyme intermediate to TEM-1 β-lactamase (*19*) indicated that the additional phenyl side group provided favorable van der Waals and hydrophobic interactions with the main chain atoms of the β-strand forming one side of the active site cavity (residues 235−238). By analogy, it was surmised that introduction of the phenylacetamido group into our boronate inhibitor should provide additional binding energy and inhibitory efficacy.

Scheme 1

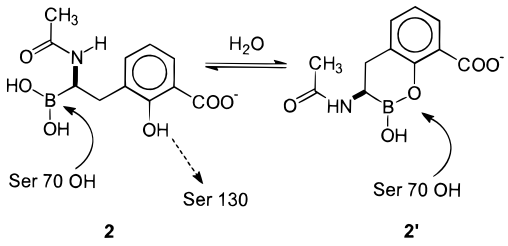

Additional improvement of the inhibitory potency of the boronate compound seemed possible by introduction of a phenolic hydroxyl group, as in compound **2** (Figure 1b). Molecular modeling of this compound indicated the potential for the energetically favorable hydrogen bond formation between this hydroxyl group in the inhibitor and the side chain oxygen of the adjacent, conserved Ser 130 (Scheme 1). Furthermore, such a group might induce cyclic boronate ester formation (Scheme 1) with a potential for influencing the binding mechanism and for providing additional information about the attack by water in the deacylation step (*19*, *24*−*34*).

EXPERIMENTAL PROCEDURES

Synthesis of (1R)-1-Phenylacetamido-2-(3-carboxyphenyl)-ethylboronic Acid (1). Starting materials were purchased from Aldrich, and nitrocefin was from Beckton Dickinson. All chromatography was on SiO_2 gel (60 Å, 230−400 mesh). Melting points and boiling points (Kugelrohr) are uncorrected. Optical rotations were measured at 589 nm on a Perkin-Elmer 243B polarimeter, NMR spectra on a Varian XL200 or XL500 spectrometer, IR spectra with a Nicolet 8210E FT-IR, Nicolet 5DX FT-IR, or Perkin-Elmer 882 spectrophotometer, and mass spectra on a Fisons 70-250S spectrometer. Elemental analyses were by Canadian Microanalytical Service Ltd. The kinetic data were obtained with a Perkin-Elmer Lambda 2 spectrophotometer equipped with a 1 cm path length thermostated cell using PECSS software.

A mixture of 3-bromobenzoic acid (27 g, 0.13 mol) and $SOCl_2$ (34 mL, 0.47 mol) was refluxed for 2 h under Ar and the excess $SOCl_2$ removed under reduced pressure. The crude product was then distilled to yield a colorless liquid (29.1 g, 99%, bp[1] 65 °C [1 mmHg)] which was dissolved in CH_2Cl_2 (50 mL), and then added dropwise with stirring to 2-amino-2-methylpropanol (25.3 mL, 0.27 mol) in CH_2Cl_2 (50 mL) under Ar at 0 °C, and the mixture was stirred at 20 °C for 2 h. The white precipitate was filtered off and washed with H_2O (50 mL), and the solid remaining was combined with that obtained by concentrating, cooling, and filtering the CH_2Cl_2 solution to give *N*-(1,1-dimethyl-2-hydroxyethyl)-3-bromobenzamide (32.2 g, 89%): mp 93−94.5 °C; IR (KBr) 1638 cm^{-1}; ^1H NMR ($CDCl_3$) δ 1.39 (6H, s), 3.67 (2H, s), 4.38 (1H, br s), 6.15 (1H, br s), 7.28 (1H, t, J_o = 8 Hz), 7.58−7.65 (2H, m), 7.84 (1H, t, J_m = 2 Hz); ^{13}C NMR ($CDCl_3$) δ 24.28 (2C), 56.37, 70.27, 122.53, 125.42, 129.97, 130.03, 134.29, 136.78, 166.79.

Thionyl chloride (16.7 mL, 0.23 mol) was added dropwise with stirring to the above bromobenzamide (17.8 g, 65

[1] Abbreviations: mp, melting point; bp, boiling point; YT, yeast tryptone.

mmol). When the vigorous reaction had subsided, the solution was poured into dry Et_2O (100 mL) with vigorous stirring and the white hydrochloride salt filtered off, neutralized with cold 20% aqueous NaOH (80 mL), and extracted with Et_2O (4 × 50 mL). The combined Et_2O extracts were dried (K_2CO_3), evaporated, and distilled to afford 2-(3-bromophenyl)-4,4-dimethyl-2-oxazoline (14.9 g, 90%): bp 85 °C (0.03 mmHg); lit. (*14*) 105−108 °C (0.05 mmHg); IR (neat) 1649 cm^{-1}; ^1H NMR ($CDCl_3$) δ 1.35 (6H, s), 4.08 (2H, s), 7.24 (1H, t, $J_o = 8$ Hz), 7.56 (1H, dt, $J_o = 8$ Hz, $J_m = 1$ Hz), 7.83 (1H, dt, $J_o = 8$ Hz, $J_m = 1$ Hz), 8.08 (1H, t, $J_m = 2$ Hz); ^{13}C NMR ($CDCl_3$) δ 28.28 (2C), 67.62, 76.37, 122.20, 126.55, 129.87, 129.64, 131.03, 133.90, 160.55.

To a mixture of $ClCH_2I$ (10.0 mL, 0.14 mol) and $B(OMe)_3$ (14.2 mL, 0.13 mol) in dry THF (125 mL) at −78 °C under Ar was added *n*-BuLi (85.6 mL of a solution 1.6 M in THF, 0.14 mol) dropwise. After 30 min, the mixture was quenched with TMSCl (19.0 mL, 0.15 mol) and allowed to warm to 20 °C and stirred overnight. The reaction mixture was then treated with (+)-pinanediol (21.3 g, 0.13 mol) dissolved in a minimum of dry Et_2O, and stirred for 3 h. The mixture was partitioned between H_2O (200 mL) and Et_2O (100 mL); the ether layer was dried ($MgSO_4$), evaporated (bath <40 °C), and chromatographed [hexanes/EtOAc (10:1) elution] to yield (+)-pinanediol chloromethylboronate as a colorless liquid (13.69 g, 78%): $[\alpha]^{25}_D = +29.2°$ ($c = 1.47$, $CHCl_3$); ^1H NMR ($CDCl_3$) δ 0.82 (3H, s), 1.12 (1H, d, $J = 11$ Hz), 1.27 (3H, s), 1.40 (3H, s), 1.8−2.4 (5H, m), 2.99 (2H, s), 4.35 (1H, dd, $J_{AX} = 2$ Hz, $J_{AY} = 9$ Hz); ^{13}C NMR ($CDCl_3$) δ 23.83, 26.25, 26.90, 28.32, 35.06, 38.07, 39.28, 51.06, 78.58, 86.91; CH_2B not seen.

n-BuLi (3.86 mL, 6.2 mmol) was added to a cold (−100 °C) solution of the above oxazoline (1.57 g, 6.17 mmol) in dry THF (20 mL), and, after stirring for 20 min, a precooled (−100 °C) solution of (+)-pinanediol chloromethylboronate (1.41 g, 6.2 mmol) in dry THF (10 mL) was added via cannula. The resulting mixture was then allowed to warm to 20 °C, then stirred overnight, evaporated, and flash chromatographed [hexanes/EtOAc (5:1) elution] to yield (+)-pinanediol (3-(4,4-dimethyl-Δ^2-oxazolino)phenyl)methylboronate as a colorless oil (1.80 g, 80%): $[\alpha]^{25}_D = +8.4°$ ($c = 1.95$, $CHCl_3$); IR (neat) 1652 cm^{-1}; ^1H NMR ($CDCl_3$) δ 0.79 (3H, s), 1.03 (1H, d, $J = 11$ Hz), 1.24 (3H, s), 1.35 (9H, s), 1.7−2.4 (5H, m), 2.34 (2H, s), 4.06 (2H, s), 4.24 (1H, dd, $J_{AX} = 2$ Hz, $J_{AY} = 9$ Hz), 7.2−7.3 (2H, m), 7.6−7.8 (2H, m); ^{13}C NMR ($CDCl_3$) δ 19.5, 23.92, 26.38, 27.00, 28.40 (2C), 28.54, 35.35, 38.04, 39.39, 51.19, 67.36, 77.86, 78.90, 85.76, 124.75, 127.81, 128.02 (2C), 131.66, 138.95, 162.11.

A solution of CH_2Cl_2 (0.17 mL, 2.7 mmol) in dry THF (4 mL) was cooled to −100 °C (95% EtOH/liquid N_2 slush bath) and cold *n*-BuLi (1.35 mL, 2.17 mmol) added dropwise with stirring during 10 min, taking care to avoid any warming. After 30 min, the above (+)-pinanediol oxazolinomethylboronate (0.758 g, 2.06 mmol) in dry THF (2 mL) was injected in one portion via cannula, resulting in the dissolution of the precipitate of Cl_2CHLi. Precipitation of the boronate adduct followed, and the solution was then allowed to warm to 20 °C and stirred for 6 h, after which time freshly prepared $LiN(TMS)_2$ [from *n*-BuLi (1.31 mL, 2.09 mmol) and $HN(TMS)_2$ (0.45 mL, 2.15 mmol) in dry THF (6 mL), reacted at −78 °C, warmed to 20 °C, and then stirred for 30 min] was added dropwise at −78 °C. The reaction mixture was then allowed to warm gradually to 20 °C and stirred overnight. It was then recooled to −78 °C and treated with $(PhCH_2CO)_2O$ (*34*) (2.23 g, 8.76 mmol) followed by glacial AcOH (0.12 mL, 2.16 mmol), and the mixture was allowed to warm to 20 °C and stirred overnight. The mixture was then evaporated and flash chromatographed (EtOAc elution). Recrystallization from EtOAc/hexanes afforded (+)-pinanediol (1*R*)-1-phenylacetamido-2-(3-(4,4-dimethyl-Δ^2-oxazolino)phenyl)ethylboronate (0.676 g, 64%): $[\alpha]^{25}_D = -39.5°$ ($c = 1.09$, $CHCl_3$); mp 121−123 °C; IR (KBr) 1652, 1609 cm^{-1}; ^1H NMR ($CDCl_3$) δ 0.87 (3H, s), 1.28 (3H, s), 1.33 (1H, d, $J = 10$ Hz), 1.38 (6H, s), 1.41 (3H, s), 1.7−2.4 (5H, m), 2.6−3.0 (3H, m), 3.61 and 3.67 (2H, d, $J_{AB} = 17$ Hz), 4.10 (2H, s), 4.28 (1H, dd, $J_{AX} = 2$ Hz, $J_{AY} = 9$ Hz), 5.83 (1H, br s), 7.00−7.36 (7H, m), 7.68−7.76 (2H, m); ^{13}C NMR ($CDCl_3$) δ 24.15, 26.44, 27.30, 28.42 (2C), 28.91, 36.18, 37.17, 38.13, 39.91, 40.23, 42.4 (1C, br m), 52.02, 67.52, 77.01, 79.05, 84.26, 126.06, 127.63, 128.28 and 128.53 (3C), 128.99 (2C), 129.31 (2C), 131.61, 132.84, 140.35, 161.85, 174.32.

The above phenylacetamidoboronate (0.559 g, 1.1 mmol) was dissolved under Ar in 3 M aqueous HCl (25 mL, prepared with degassed H_2O) and refluxed for exactly 1 h with a preheated oil bath. The solution was then cooled to 20 °C and washed with Et_2O (4 × 20 mL). The aqueous phase was then evaporated under high vacuum at 25 °C, using a NaOH trap, to yield the (1*R*)-1-phenylacetamido-2-(3-carboxyphenyl)ethylboron dichloride 2-amino-2-methyl-1-propanol salt (0.53 g, quant.) which was converted to (1*R*)-1-phenylacetamido-2-(3-carboxyphenyl)ethylboronic acid (**1**) by repeated recrystallization from aqueous acetone: mp 210 °C dec (anhydride); $[\alpha]^{25}_D$ −112.2° ($c = 0.09$, H_2O); IR (KBr) 1701, 1602 cm^{-1}; ^1H NMR (DMSO-d_6) δ 2.46−2.50 (1H, m), 2.68−2.77 (2H, m), 3.53 (2H, m), 7.13−7.36 (8H, m), 7.72−7.77 (2H, m), 8.73 (1H, br s), 12.79 (1H, br s); ^{13}C NMR (DMSO-d_6) δ 36.56, 38.31, 46.70 (1C, br m), 126.45, 126.62, 128.01, 128.21 (2C), 128.93 (2C), 129.77, 130.41, 133.34, 134.57, 141.69, 167.48, 173.53; Anal Calcd for dimer anhydride $C_{34}H_{34}B_2N_2O_9$: C, 64.18; H, 5.39; N, 4.40; B, 3.40. Found: C, 64.47; H, 5.20; N, 4.86; B, 3.37.

*Synthesis of (1R)-1-Acetamido-2-(3-carboxy-2-hydroxyphenyl)ethylboronic Acid (**2**).* A solution of 2-methylphenol (34.4 mL, 0.33 mol) and sulfuric acid (31.0 mL, 96%) was heated to 110 °C for 2 h and then cooled to 10 °C, and nitrobenzene (84.0 mL) and sulfuric acid (11.0 mL, 43%) were added. A solution of Br_2 (19.3 mL, 0.38 mol) in nitrobenzene (42.0 mL) was added dropwise over 2 h at 5 °C. The crude product was subjected to steam distillation at 230 °C bath temperature, extracted, and distilled (15 mbar, 15 cm Vigreux column) to yield 3-bromo-2-methylphenol (34.1 g, 56%): bp 107−109 °C/15 mmHg; IR (neat) 3513, 1125 cm^{-1}; ^1H NMR ($CDCl_3$) δ 7.28 (1H, d), 7.09 (1H, d), 6.71 (1H, t), 5.56 (1H, s), 2.30 (3H, s); ^{13}C NMR ($CDCl_3$) δ 150.3, 130.9, 130.3, 129.1, 121.1, 110.1, 16.5.

To a solution of 3-bromo-2-methylphenol (34.0 g, 0.18 mol), dissolved in refluxing water (67.0 mL), were added, in parallel, $(CH_3)_2SO_4$ (34.3 mL) and KOH (30.6 g, 0.55 mol) in water (30.0 mL). The crude product was distilled to yield 3-bromo-2-methoxytoluene (29.2 g, 80%): bp 120−125 °C/15 mbar; IR (film) 1470, 1230, 1011 cm^{-1}; ^1H NMR ($CDCl_3$) δ 7.37 (1H, d, $J_o = 8.2$ Hz), 7.15 (1H, d, $J_o = 8.3$

Hz), 6.88 (1H, t, J_o = 7.7 Hz), 3.81 (3H, s), 2.33 (3H, s); ^{13}C NMR ($CDCl_3$) δ 155.2, 133.0, 130.9, 130.4, 125.0, 117.6, 59.9, 16.4.

To a refluxing solution of 3-bromo-2-methoxytoluene (29 g, 45 mmol) and NaOH (6 g, 150 mmol) in water (1.5 L) was added $KMnO_4$ (85 g, 536 mmol). After 2 h, the mixture was cooled to 25 °C and stirred for a further 18 h. Sodium bisulfite was added until decolorization was complete, and the mixture was acidified with concentrated H_2SO_4. The precipitate was filtered off, then redissolved in 2 M aqueous NaOH (150 mL), and extracted with CH_2Cl_2 (2 × 20 mL). The aqueous phase was acidified with 6 M HCl (10%), and the precipitate was filtered off and dried to yield 3-bromo-2-methoxybenzoic acid (20.2 g, 61%): mp 120−122 °C; IR (KBr) 1681, 1456, 1360 cm^{-1}; ^{1}H NMR (DMSO-d_6) δ 7.82 (1H, d, J_o = 7.8 Hz), 7.69 (1H, d, J_o = 7.7 Hz), 7.15 (1H, t, J_o = 7.8 Hz), 3.80 (3H, s); ^{13}C NMR (DMSO-d_6) δ 166.4, 155.5, 136.5, 130.3, 128.2, 125.5, 118.0, 61.7.

A mixture of 3-bromo-2-methoxybenzoic acid (10.1 g, 43.8 mmol) and $SOCl_2$ (11 mL, 150 mmol) was heated to 80 °C and distilled to yield the acid chloride [10.6 g, 97%, bp 82 °C (0.002 mmHg)], which was then dissolved in CH_2Cl_2 (15 mL) and added with stirring to a solution of 2-amino-2-methyl-3-hydroxypropane (7.57 g, 85 mmol) in dry CH_2Cl_2 (20 mL) at 0 °C. After stirring for a further 2 h, the residue was filtered off and the organic phase evaporated to yield *N*-(1,1-dimethyl-2-hydroxyethyl)-3-bromo-2-methoxybenzamide (12.6 g, 98%): mp 96 °C; IR (KBr) 1642, 1454, 1303 cm^{-1}; ^{1}H NMR ($CDCl_3$) δ 7.93 (1H, dd, J_o = 7.9 Hz, J_m = 1.8 Hz), 7.63 (1H, dd, J_o = 7.9 Hz, J_m = 1.7 Hz), 7.08 (1H, t, J_o = 7.9 Hz), 4.81 (1H, t, J = 5.9 Hz), 3.86 (3H, s), 3.66 (2H, d, J = 5.9 Hz), 1.38 (6H, s); ^{13}C NMR ($CDCl_3$) δ 164.6, 154.5, 136.6, 130.7, 128.8, 126.0, 117.7, 70.4, 61.8, 56.1, 24.5.

To *N*-(1,1-dimethyl-2-hydroxyethyl)-3-bromo-2-methoxybenzamide (12.6 g, 42 mmol) was added $SOCl_2$ (12.4 g, 104 mmol) and the mixture then poured into Et_2O and stirred vigorously for 1 h. The precipitate was filtered off, washed with Et_2O (50 mL), and dissolved in 10% aqueous NaOH (50 mL). After workup, 2-(3-bromo-2-methoxyphenyl)-4,4-dimethyl-2-oxazoline (**9**) (10.8 g, 91%) was obtained: IR (KBr) 1646, 1463, 1249, 1062 cm^{-1}; ^{1}H NMR ($CDCl_3$) δ 7.66 (1H, dd, J_o = 7.8 Hz, J_m = 1.6 Hz), 7.60 (1H, dd, J_o = 7.9 Hz, J_m = 1.8 Hz), 6.96 (1H, t, J_o = 7.9 Hz), 4.08 (2H, s), 3.83 (3H, s), 1.35 (6H, s); ^{13}C NMR ($CDCl_3$) δ 159.8, 155.9, 135.6, 130.2, 124.6, 124.0, 118.4, 78.8, 67.5, 61.4, 28.0.

To 2-(3-bromo-2-methoxyphenyl)-4,4-dimethyl-2-oxazoline (**3**, 2.82 g, 10 mmol) in THF (20 mL) at −90 °C was added *n*-BuLi (7 mL, 11 mmol). (+)-Pinanediol chloromethylboronate (2.28 g, 10 mmol) in THF (10 mL, cooled to −90 °C) was then added via cannula and the reaction mixture warmed to 25 °C and stirred for 18 h. The solution was rotoevaporated at 20 °C and chromatographed (400 g of SiO_2, hexanes/EtOAc, 10:1 gradient to 1:1) to yield (+)-pinanediol (3-(4,4-dimethyl-Δ^2-oxazolino)-2-methoxyphenyl)methylboronate (**4**) (2.16 g, 54%): mp 69 °C; $[\alpha]_D^{25}$ = +9.26° (c = 2.18, $CHCl_3$); IR (KBr) 1640, 1470, 1338, 1066 cm^{-1}; ^{1}H NMR ($CDCl_3$) δ 7.53 (1H, dd, J_o = 8.0 Hz, J_m = 1.1 Hz), 7.01 (1H, dd, J_o = 7.5 Hz, J_m = 1.1 Hz), 7.30 (1H, t, J_o = 7.4 Hz), 4.28 (1H, d, J = 7.8 Hz), 4.10 (2H, s), 3.79 (3H, s), 2.36 (2H, s), 2.22 (1H, m), 2.03 (1H, t, J = 5.2 Hz), 1.85 (2H, m), 1.39 (6H, s), 1.37 (3H, s), 1.27 (3H, s), 1.13 (2H, d, J = 10.9 Hz), 0.82 (3H, s); ^{13}C NMR ($CDCl_3$) δ 160.76, 156.66, 133.06, 132.96, 127.85, 122.83, 121.27, 85.16, 78.34, 77.34, 66.79, 60.66, 50.81, 38.97, 37.58, 34.91, 28.09, 27.83, 26.56, 25.86, 23.45, 13.10.

n-BuLi (3.16 mL of 1.6 M in hexanes, 5.1 mmol) was added dropwise to a solution of CH_2Cl_2 (419 μL, 6.54 mmol) in THF (10 mL) at −100 °C. After 15 min at this temperature, (+)-pinanediol (3-(4,4-dimethyl-Δ^2-oxazolino)-2-methoxyphenyl)methylboronate (**4**, 2 g, 5 mmol) in THF (6 mL) was added via cannula. The reaction mixture was warmed to 25 °C and stirred for 6 h. LHMDS (5.4 mmol) in THF (5 mL) was added at −78 °C, and the reaction was stirred for 18 h at 25 °C. $(CH_3CO)_2O$ (2 mL, 21 mmol) and glacial CH_3COOH (300 μL, 5.2 mmol) were added at −78 °C. The solution was warmed to 25 °C and stirred for 18 h, and then evaporated, and the residue was chromatographed (Et_2O/MeOH, 10:1) to yield (+)-pinanediol (1*R*)-1-acetamido-2-(3-(4,4-dimethyl-Δ^2-oxazolino)-2-methoxyphenyl)ethyl boronate (**5**, 1.39 g, 60%): mp 176 °C (dec); $[\alpha]_D^{25}$ = −70.34 (c = 3.24, $CHCl_3$); IR (KBr) 3416, 1651, 1623, 1152 cm^{-1}; ^{1}H NMR ($CDCl_3$) δ 7.58 (1H, dd, J_o = 7.7 Hz, J_m = 1.8 Hz), 7.27 (1H, dd, J_o = 7.6 Hz, J_m = 1.8 Hz), 7.05 (1H, t, J_o = 7.7 Hz), 6.95 (1H, bs), 4.21 (1H, dd, J = 8.67 Hz, J = 8.42 Hz), 4.08 (2H, s), 3.74 (3H, s), 2.86 (3H, s), 2.30 (1H, m), 2.15 (1H, m), 2.05 (3H, s), 1.98 (1H, m), 1.86 (2H, m), 1.48 (1H, d, J = 10.1 Hz), 1.39 (3H, s), 1.38 (6H, s), 1.26 (3H, s), 0.82 (3H, s); ^{13}C NMR ($CDCl_3$) δ 174.55, 160.77, 157.33, 135.19, 133.47, 129.21, 123.55, 121.67, 82.79, 78.59, 76.04, 67.37, 61.33, 52.17, 44.80, 39.82, 37.84, 36.50, 32.12, 28.98, 27.99, 27.86, 27.12, 26.29, 23.96, 17.97, 13.88.

To the protected boronic acid **5** (661 mg, 1.4 mmol) was added BCl_3 (1 M in CH_2Cl_2, 8 mL, 8 mmol) at −100 °C, and the solution was then warmed to 25 °C and stirred for 18 h. The solvent was then evaporated, MeOH (5 mL) added, the mixture refluxed for 10 min, and the solvent rotoevaporated again. This process was repeated 4 times. The residue was then treated with 6 M HCl (10 mL) and refluxed for 24 h and cooled, and the mixture was extracted with Et_2O (4 × 5 mL) and the aqueous phase evaporated. The residue was stirred in water (25 mL) for 18 h and the precipitate filtered and dried to yield (1*R*)-1-acetamido-2-(3-carboxy-2-hydroxyphenyl)ethylboronic acid (**2**, 30 mg, 11%): mp 274 °C dec (anhydride); $[\alpha]_D^{25}$ = +39.7° (c = 0.6, DMSO); IR (KBr) 3350, 1678, 1580, 1380, 1255, 1140, 1080 cm^{-1}; ^{1}H NMR (DMSO-d_6) δ 10.24 (1H, d, J = 27.2 Hz), 7.70 (1H, d, J_o = 7.8 Hz), 7.28 (1H, d, J_o = 7.3 Hz), 6.90 (1H, t, J_o = 7.3 Hz), 4.79 (0.5H, bs), 3.33 (1H, s), 3.18 (1H, m), 2.80 (2H, m), 2.04 (1H, m), 1.94 (3H, m), 1.56 (3H, s), 1.55 (3H, s); ^{13}C NMR (DMSO-d_6) δ 177.02 + 176.82, 166.03, 156.04 + 156.33, 134.67, 129.32, 127.27, 120.18, 117.29 + 117.20, 45.47, 31.13, 15.83 + 15.75; ^{11}B NMR (DMSO) δ 16, HWB = 27 ppm; Calcd for $C_{11}H_{14}BNO_6$: C, 49.48; H, 5.28; N, 5.25; B, 4.05. Found: C, 49.09; H, 5.00; N, 5.01; B, 3.60.

Enzyme Purification. *E. coli* MV1183 transformed with pUC118 (*36*) was grown at 37 °C in 2×YT medium with shaking to A_{660} = 3.3; then 600 mL of culture was centrifuged at 5 °C for 20 min at 12 000 rpm and the pellet resuspended in 10 mL of 30 mM Tris-HCl, pH 7.5, 1 mM NaEDTA. This paste was rapidly squirted via a 10 mL pipet into 300 mL of cold, rapidly stirred, 0.1 mM $ZnCl_2$/0.1 mM

$MgCl_2$. After 30 min, the lysate was centrifuged for 40 min at 12 000 rpm to remove debris. An 11 × 1.8 cm column of Q-Sepharose FastFlow (Pharmacia) was prepared and equilibrated with 30 mM Tris-HCl, pH 8.0, and 150 mL of lysate was applied to the column, which was developed with a linear gradient (200 mL) of NaCl (0−1 M) in equilibration buffer. The flow rate was 4 mL/min, and 10 mL fractions were collected. Each fraction was assayed for activity by a colorimetric method using 7-(thienyl-2-acetamido)-3-[2-(4-*N*,*N*-dimethylphenylazo)pyridiniummethyl]-3-cephem-4-carboxylic acid (PADAC). Protein content was visualized by SDS−PAGE. Active fractions which appeared to be homogeneous after Coomassie Blue staining were obtained which, when stored at −20 °C, retained full activity for up to 6 months. The yield was 45 mg of protein of specific activity 3.7 mmol·min^{-1}·mg.

Kinetic Measurement of β-Lactamase TEM-1 Inhibition. The kinetic measurements were performed in duplicate by the initial rate method in 3 mL, 1 cm path length, quartz cuvettes and monitoring absorbance changes at 482 nm [$\epsilon = (1.980 \pm 0.004) \times 10^4$ cm^{-1} M^{-1}] with nitrocefin as substrate in the concentration range 10−300 μM in 50 mM NaH_2PO_4 buffer (5% DMSO, pH 7.0) at 25 °C. The reactions were initiated by addition of enzyme (10.0 μL), followed by rapid mixing, and after a 5 s delay to attain homogeneity, the absorbance changes were recorded for 300 s. The enzyme stock solution (in 5% DMSO) was diluted to give reasonable slopes in the desired substrate concentration range [(∼0.2−4)K_M]. The corrected substrate concentrations and calculated slopes (with the PECSS software) for less than 5% conversion were then introduced into the GraFit program (Erithacus Software Ltd., Staines, U.K.), and nonlinear regression curve-fitting was used to calculate $K_M = (2.55 \pm 0.05) \times 10^{-5}$ M, $V_{max} = (2.05 \pm 0.02) \times 10^{-8}$ M s^{-1}.

The K_I's for **1** and **2** were then obtained by comparison of progress curves in the presence, and absence, of inhibitor, as described by Waley (*37*). The enzyme was preincubated with the inhibitor for 10 min and the substrate added last to initiate the reaction. Sufficient inhibitor was used to give at least 50% inhibition. Typical stock solutions of inhibitors contained 1 mg of inhibitor/mL of buffer. After initiation of the reaction, a waiting period of 15 s for consistency was applied, followed by recording the progress curves for 500 s. The K_I's of 5.9 ± 0.1 nM for **1** and 13 ± 2 nM for **2** were calculated by the Waley protocol (*38*, *39*).

Structure Determination. Native TEM-1 β-lactamase was expressed and isolated from cultures of *E. coli* carrying the plasmid pUC118 (*36*). Orthorhombic crystals of native TEM-1 were grown in 1.5 M phosphate, pH 8.0 (*19*). A quantity of each inhibitor determined to yield a 2:1 molar ratio with the enzyme was dissolved in mother liquor and then soaked into the native crystal for a period of 6 h. For compound **2**, data to 2.1 Å were collected at room temperature using an R-axis II Image Plate Detector mounted on a Rigaku rotating anode running at 50 kV, 150 mA. Data processing was accomplished using the software Denzo (*40*). The merging *R* on intensities for 94 712 observations of 17 781 unique reflections was 0.042. For compound **1**, data to 1.9 Å resolution were collected using a Quanta 4 CCD detector at beamline X12B at the NSLS, Brookhaven National Laboratory. The merging *R* on intensities for 73 805 observations of 18 128 unique reflections is 0.069. Refinement and model building was performed as described below. Restraints on bond distance, angles, and planarity of the phenylacetamido ring were applied to the inhibitor during refinement. No torsional angles were restrained in the refinement. Coordinates have been deposited in the Protein Data Bank under the numbers 1ERM, 1ERO, and 1ERQ (*41*).

Scheme 2[a]

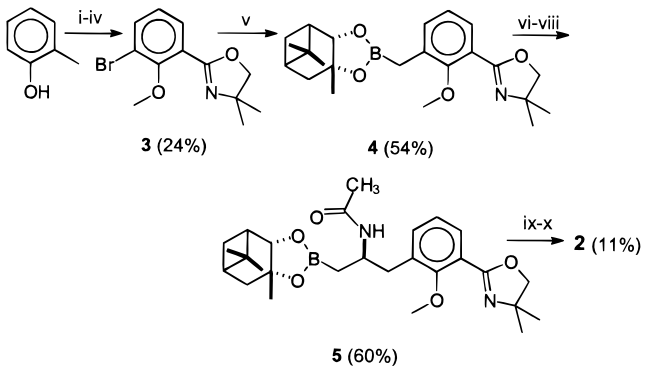

[a] i: H_2SO_4, Br_2; ii: KOH, Me_2SO_4; iii: NaOH, $KMnO_4$; iv: $SOCl_2$, $C_4H_{11}NO$; v: *n*-BuLi, $ClCH_2BO_2R$*; vi: $LiCHCl_2$; vii: $LiN(SiMe_3)_2$; viii: Ac_2O, AcOH; ix: BCl_3; x: 6 N HCl.

RESULTS AND DISCUSSION

Synthesis. The synthetic sequence to (1*R*)-1-phenylacetamido-2-(3-carboxyphenyl)ethylboronic acid (**1**) is based on the methodology developed by the Matteson (*42*) and Kettner (*43*) groups, and followed the approach reported for the previously characterized boronic acid variant (1*R*)-1-acetamido-2-(3-carboxyphenyl)ethaneboronic acid (**3** in Figure 1) (*23*, *24*). Using 3-bromobenzoic acid as starting material, inhibitor **1** was obtained in an overall yield of 40%.

The synthetic sequence used to obtain (1*R*)-1-acetamido-2-(3-carboxy-2-hydroxyphenyl)ethylboronic acid (**2**), whose substitution pattern is not easily achievable (*44*), is shown in Scheme 2. Bromination of *o*-cresol (*45*) was followed by protection of the hydroxyl group as a methyl ether (*46*), the alternative *tert*-butyl ether protection approach having been unsuccessful (*47*). In contrast to previous reports (*44*), subsequent oxidation of the methyl group to the carboxylic acid by alkaline $KMnO_4$ proceeded smoothly. Protection of the carboxylic acid as an oxazoline (*48*) gave intermediate **3** in acceptable overall yield. Li−Br exchange, using *n*-BuLi at −100 °C, followed by coupling with (+)-pinanediolchloromethane boronate (*49*), afforded the protected boronate ester **4**. This was then homologated with dichloromethyllithium to give the α-chloroboronate ester, which was reacted in situ with freshly prepared lithium hexamethyldisilazane. The resulting, unstable, silylated aminoboronate was subsequently acylated with excess acetic anhydride and an equimolar amount of acetic acid to give α-amido boronic ester **5**. Subsequent deprotection with BCl_3 and then refluxing in 6 M HCl yielded the target inhibitor **2**.

Interestingly, although boronic acids can suffer from hydrolytic, protonolysis, and autoxidation complications (*50*), internal complexation of the carbonyl oxygen of the *N*-acyl side chain with the boron atom for **1** and **2** appears to protect against such damage during the final steps of Scheme 2-like reactions. Such complexation was indicated in the IR spectra by the lower-than-normal amide absorption frequencies of the *N*-acyl carbonyl groups of **1**. Similar 1-acetamidoalkyl-

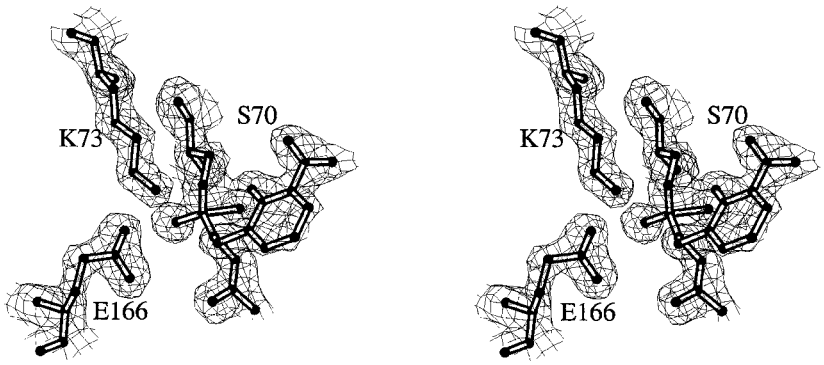

FIGURE 2: Stereographic view of the final 1.9 Å $2|F_o| - |F_c|$ electron density map of (1*R*)-1-acetamido-2-(3-carboxyhydroxyphenyl)-ethylboronic acid (**2**) contoured at 2.0σ in the region of the active site.

boronic acid compounds also showed complexation by X-ray crystallography (*51*). Furthermore, the *N*-acyl functionality of **2** is more stable toward acidic conditions than for **1**. This is presumably due to internal boronic acid ester formation, as outlined in Scheme 1, which prevents the Lewis acid-catalyzed hydrolysis of the acetamide by the boron atom, as well as the other complications (*50*) mentioned above.

Kinetic Evaluations. Kinetic evaluation (*37*) of transition state analogue inhibitors **1** and **2** confirmed that, as designed, they were highly effective competitive inhibitors of class A TEM-1 β-lactamase, exhibiting encouragingly low nanomolar inhibition constants. The strong binding of **1**, with its K_I of 5.9 nM, is 19-fold lower than that of the *N*-acetyl analogue (compound **3** in Figure 1; K_I of 110 nM) (*23*), due to the much more hydrophobic phenylacetamido function. The phenolic boronic acid **2** is also a very powerful inhibitor, with a K_I of 13 nM. This represents a 8.5-fold stronger binding than for its *N*-acetyl analogue (compound **3**), thereby confirming the validity of the concept of exploiting additional H-bonding interactions in the design of more powerful inhibitors.

The affinities of boronic acid inhibitors **1** and **2** match those of the most powerful mechanism-based inhibitors, such as penem BRL 42715 and olivanic acid derivatives (*51*−*53*). To our knowledge, inhibitors **1** and **2** appear to be among the most powerful transition state analogue inhibitors of a β-lactamase yet reported. Importantly, however, it should be noted that transition state analogue phosphonate esters and phosphonamidates are also extremely potent inhibitors of β-lactamases (*55*−*59*).

X-ray Crystallographic Structure Determination. The crystallographic structures of the complex of TEM-1 β-lactamase from *E. coli* and inhibitors **1** and **2** were pursued by soaking the compounds at a concentration of 5 mM for 6 h into the previously described orthorhombic ($P2_12_12_1$) crystal form of the enzyme (*19*). Figure 2 shows the final $2|F_o| - |F_c|$ electron density for the (1*R*)-1-acetamido-2-(3-carboxy-2-hydroxyphenyl)ethylboronic acid (compound **2**) inhibitor bound to TEM-1 β-lactamase. The initial difference Fourier electron density for this complex unambiguously verified the covalent link of the boron atom to the Oγ side chain oxygen of the Ser70 nucleophile and the formation of a tetrahedral stereochemistry at the boronate center which mimics the transition state of deacylation in the class A β-lactamase reaction (the boron atom can be considered analogous to the C7 atom of the β-lactam substrate). The model for the inhibitor was constructed using the previously determined 1.7 Å structure of (1*R*)-1-acetamido-2-(3-carboxyphenyl)-ethaneboronic acid (*24*) (compound **3** in Figure 1) covalently bound to TEM with verification provided from structures from the Cambridge Structural Database (CSD, Version 4, 1988). Least-squares refinement was performed using TNT (*60*) with the inhibitor at full occupancy. The final *R*-factor for the complex using all data from 20 to 1.9 Å is 19.1%.

Table 1: Crystallographic Statistics for Inhibitors **1** and **2**

	inhibitor **1**	inhibitor **2**
refinement statistics		
resolution range (Å)	20.0−2.1	20.0−1.9
$R = (\sum\|F_o\| - \|F_c\|/\sum\|F_o\|)$	0.181	0.191
no. of unique reflections	11762	18087
no. of protein atoms	2018	2018
no. of solvent atoms	62	127
rms deviations from ideal values		
bond distance (Å)	0.010	0.009
trigonal planes (Å)	0.012	0.012
bond angles (deg)	2.0	1.9
general planes (Å)	0.012	0.010
av overall *B*-factors (Å)		
protein	29.7	25.9
inhibitor	25.6	25.0

For (1*R*)-1-phenylacetamido-2-(3-carboxyphenyl)ethylboronic acid (compound **1**; Figure 1b), the crystallographic cell had changed sufficiently from native TEM-1 such that molecular replacement was performed with the program EPMR [Evolutionary Programming for Molecular Replacement (*61*)]. A rotation and translation solution was easily obtained, and first maps were constructed. The initial difference electron density for compound **1** indicated less than full occupancy for the inhibitor. The addition of the phenyl moiety makes compound **1** considerably more hydrophobic, and thus the solubility of the compound was likely diminished in our 1.8 M phosphate crystallization conditions. Various occupancy levels were tried in the refinement protocol, and the final occupancy of compound **1** was reduced to 0.50. The final crystallographic refinement statistics for both compounds are summarized in Table 1.

Structure Description. Figure 3C is a detailed view of the active site of TEM and the inhibitor (1*R*)-1-acetamido-2-(3-carboxy-2-hydroxyphenyl)ethylboronic acid (compound **2**). The transparent surface shown was created with the software PREPI, with a probe radius of 2.0 Å. As designed, the tetrahedral boronic acid−enzyme adduct positions one oxygen (OH1) in the oxyanion hole formed by the main chain nitrogens of Ser70 and Ala237, displacing a highly ordered

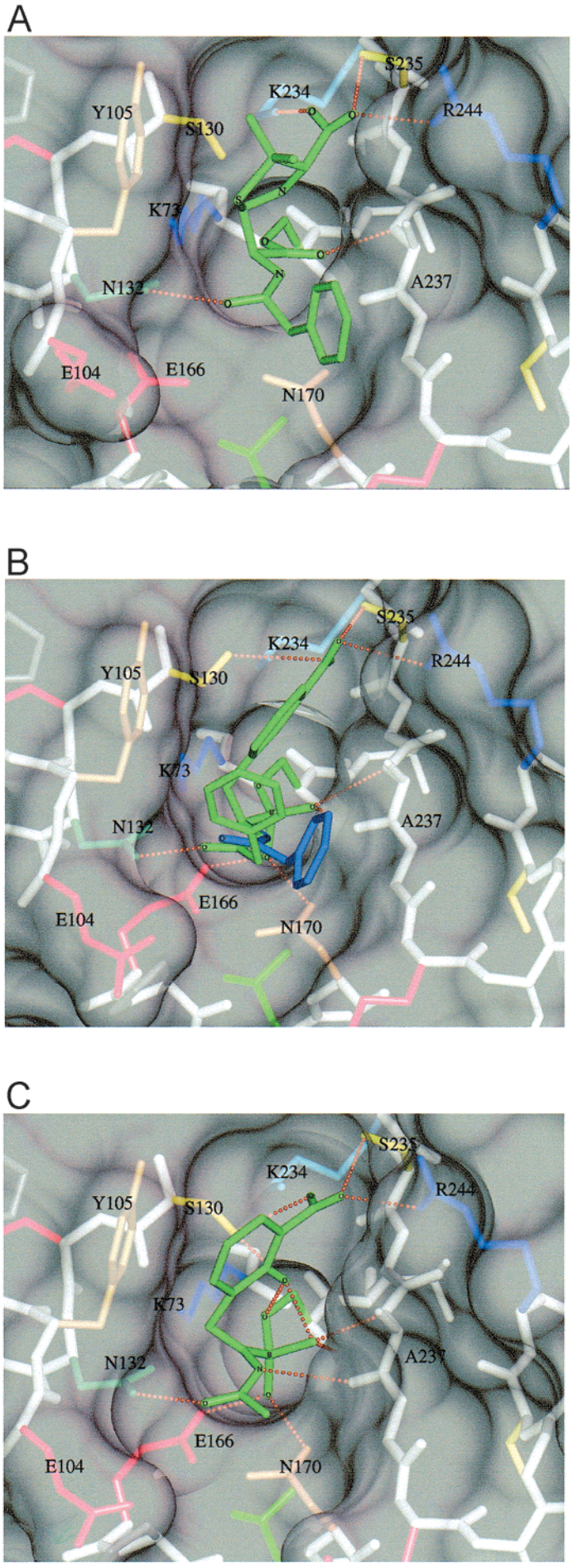

water observed in this position in all of the previously determined class A native enzymes (*19*, *30*−*34*). The second oxygen of the boronate center (OH2) hydrogen bonds to Glu166 and Asn170, displacing the highly conserved deacylating water observed in this exact position in all of the previously determined class A native enzymes (*19*, *30*−*34*). As such, these interactions mimic those expected in the deacylation tetrahedral intermediate II of the enzyme (*23*). In the earlier structure of the *N*-acetyl derivative (compound **3**) in complex with TEM-1, we observed the formation of a strong hydrogen bond (2.8 Å) between Lys73 and Glu166 which was not observed in either the native or the acyl-enzyme structures (*23*). It was suggested this provided evidence for an intermediary role of Lys73 in regenerating the Ser70 nucleophile via proton transfer from the general base of deacylation, Glu166. The distance of Glu166 to Ser70 in both the native and inhibitor-bound structures is more than 4 Å, and thus, barring significant conformational changes, a direct transfer between the two residues seems unlikely. In the structure of the higher affinity boronate compound **2** presented here, we also observe a similar formation of a strong hydrogen bond between Lys73 and Glu166 (2.7 Å), providing additional support for the role of Lys73 in the deacylation step of the catalytic mechanism.

As designed, the carboxylate of the inhibitor mimics the position of the carboxylate in the PenG substrate (*19*) (Figure 3A,C), forming strong electrostatic and hydrogen bonding interactions with the side chains of the conserved Arg244, Lys234, and Ser235 in the enzyme active site (Table 2). The side chain amide of **2** also mimics the interactions observed in the substrate, forming hydrogen bonds to the main chain carbonyl at Ala237 and the side chain amide nitrogen of the conserved Asn132.

There are also several favorable van der Waals interactions between the aromatic side chain of Tyr105 and the hydroxyphenyl group of inhibitor **2**. An analogous interaction is observed between Tyr105 and the thiazolidine ring of penicillin G (*19*). The unique hydroxyl group on the hydroxyphenyl moiety in **2** also forms a strong hydrogen bond to the Oγ of Ser130, as predicted from the modeling used in the design process. A comparison of the structure of inhibitor **2** to that observed in the previously described structure of TEM-1 bound to (1*R*)-1-acetamido-2-(3-carboxyphenyl)ethylboronic acid (compound **3**; K_i = 110 nM) (*24*) shows the two inhibitor structures superimpose very well, except for an unanticipated rotation in the hydroxyphenyl ring in compound **2** of 25.6° (Figure 4). This rotation brings the oxygen atom OH3 of the inhibitor into hydrogen bonding

FIGURE 3: Combined transparent molecular surface and ball-and-stick representation of the active site of TEM-1 β-lactamase in complex with (A) the penicillin G substrate, (B) (1*R*)-1-phenylacetamido-2-(3-carboxyphenyl)ethylboronic acid (compound **1**), and (C) (1*R*)-1-acetamido-2-(3-carboxyhydroxyphenyl)ethylboronic acid (compound **2**). Note that the E166N mutation shown in (A) was required to trap the penicillin G substrate acyl-enzyme intermediate. The alternate conformation of the phenylacetamido group in (1*R*)-1-phenylacetamido-2-(3-carboxyphenyl)ethylboronic acid (compound **1**) is shown in blue (B). Hydrogen bonds are shown as dotted lines. Main chain atoms are white, side chains atoms are colored differentially according to type, and the substrate or inhibitor atoms are shown in green. For numbering of the inhibitor atoms, see Figure 4. The figure was generated with the software package PREPI (http://bonsai.lif.icnet.uk/people/suhail/prepi.html).

Table 2: Hydrogen Bonding Distances (→) in the Inhibitor/Enzyme Complexes

location	inhibitor atom	enzyme atom	distance (Å) compd **1**	compd **2**	compd **3**
carboxylate	O3	Ser130 OG	3.5	3.4	2.5
		Ser235 OG	2.3	2.8	2.9
	O4	Ser235 OG	3.1	3.3	2.8
		Arg244 N	3.3	2.8	2.8
oxyanion hole	OH1	Ser70 N	2.9	2.8	2.7
water		Ala237 N	3.4	3.1	3.0
deacylating water	OH2	Glu166 OE1	2.6	2.9	2.5
		Asn170 OD1	2.6	2.8	2.7
side-chain amide	N1	Ala237 O	3.5 (3.3)[a]	3.2	3.3
	O2	Asn132 ND2	2.5 (3.5)[a]	2.9	2.9
hydroxyl on phenyl	OH3	Ser130 OG		2.7	
		Ser70 OG		2.3	
		Ser70 OH1		2.3	

[a] The values in parentheses are for the alternate side-chain conformation observed in compound **1**.

position with the Oγ of residue 70, the OH1 atom of the inhibitor, as well as the previously mentioned Oγ of Ser130 (Table 2). In the structure of (1*R*)-1-acetamido-2-(3-carboxyphenyl)ethylboronic acid, the phenyl ring is at a torsion angle of 82.3°, close to the theoretical most energetically favorable conformation of 90°. The hydrogen bonds from OH3 in the hydroxyphenyl variant stabilize the phenyl ring in this strained conformation, allowing the phenyl to form more favorable van der Waals interactions with the aromatic side chain of Tyr105. Together the additional interactions and conformational changes induced by the hydroxyl group likely contribute to the higher inhibitory efficacy of compound **2** relative to compound **3**.

We find no crystallographic evidence for the formation of the second cyclized boronate variant of compound **2** (Scheme 1). Instead, a strong hydrogen bond is observed between the Oγ of Ser70 and the OH1 atom of the inhibitor. In addition, there is a strong hydrogen bond from OH1 to the Oγ of Ser130. All trials of refinement in which the appropriate restraints and coordinates for a cyclized model were input into the existing data resulted in distances and angles between the relevant atoms (Scheme 1) which were incompatible with a covalent linkage (>2.3 Å) and suggestive instead of strong hydrogen bonding interactions.

The high-resolution structure of (1*R*)-1-phenylacetamido-2-(3-carboxyphenyl)ethylboronic acid (**1**) bound to TEM-1 β-lactamase shows, again as designed, a very similar set of interactions between inhibitor and enzyme as observed in compounds **2** and **3** and the PenG substrate (Figure 3, Table 2). The predominant difference in compound **1** is of course the addition of the phenylacetamido side chain (Figures 1b and 3B). The aromatic moiety adopts two conformations of approximately equal occupancy. One conformation mimics that observed in the PenG substrate (*19*) (Figure 3A), forming van der Waals interactions with the edge β-strand of the enzyme active site (residues 235−238). This conformation is shown in blue in Figure 3B. The second conformation of the side chain phenylacetamido group was unanticipated in our modeling studies and arises from a favorable aromatic stacking interaction of the side chain aromatic group and the phenyl group carrying the carboxylate of the inhibitor and Tyr105 in the enzyme (Figure 3B). Refinement trials

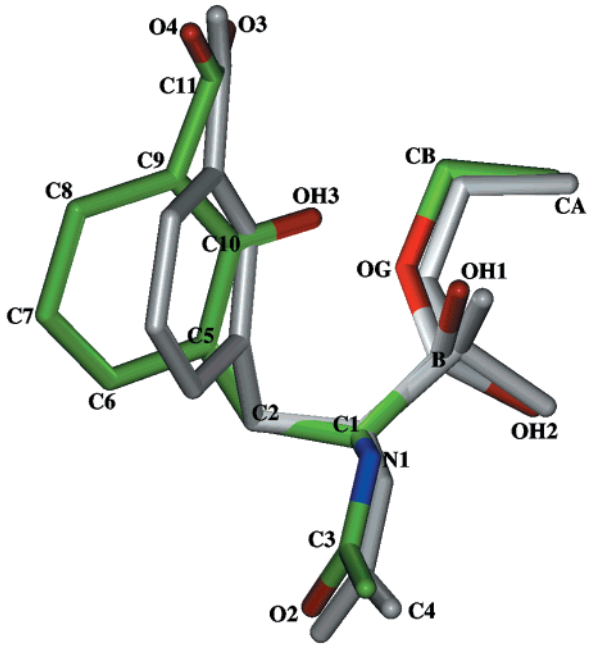

FIGURE 4: Overlap of the boronate inhibitors (1*R*)-1-acetamido-2-(3-carboxyhydroxyphenyl)ethylboronicacid (**2**) and (1*R*)-1-acetamido-2-(3-carboxyphenyl)ethaneboronic acid (**3**), highlighting the unanticipated rotation in the hydroxyphenyl ring of compound **2**. Atoms are labeled according to their reference in the text.

indicate that these two conformations exist with approximately equal occupancy in the complex.

Conformational Changes in the Position of Active Site Residues. The three polypeptide chains of TEM-1 complexed with inhibitors **1**, **2**, and **3** superimpose very closely on each other, as well as with the native enzyme (root-mean-square deviations range from 0.17 to 0.24 Å for all α-carbon atoms). There are very few differences in main chain positions, and the only significant differences in side chain positions are observed in the active site residues Tyr105, Ser130, and Glu104 that surround the inhibitor binding site (rmsd values range from 0.32 to 0.48 Å for all-atom superpositions of the native and the three inhibitors). The small changes observed in these side chain positions reflect the unique nature of each boronate compound. The interactions of Tyr105 (van der Waals) and Ser130 (hydrogen bonding) with inhibitor are affected by the addition of the hydroxyl on the phenyl group in compound **2**. Similarly, the van der Waals interactions of Tyr105 and Glu104 with inhibitor are likely affected by the conformation of the bulky phenylacetamido side group in compound **1**.

Displacement of Ordered Water To Facilitate Inhibitor Binding. Waters play an important entropic role in the binding of inhibitors to TEM (*23*). The boronate inhibitors were designed to displace two ordered waters (the deacylating water and the oxyanion hole water) found in a conserved location within the active site of TEM and all other group 2b β-lactamases for which structural information exists. Both of these waters are displaced by the inhibitor in all three boronate complexes as described above. In addition, there is an additional significant displacement of water caused by the phenylacetamido side chain moiety in the high-affinity compound **1**. Figure 5 shows an overlap of compounds **1**, **2**, and **3** along with the corresponding ordered water molecules present in each of the crystallographic structures of the native

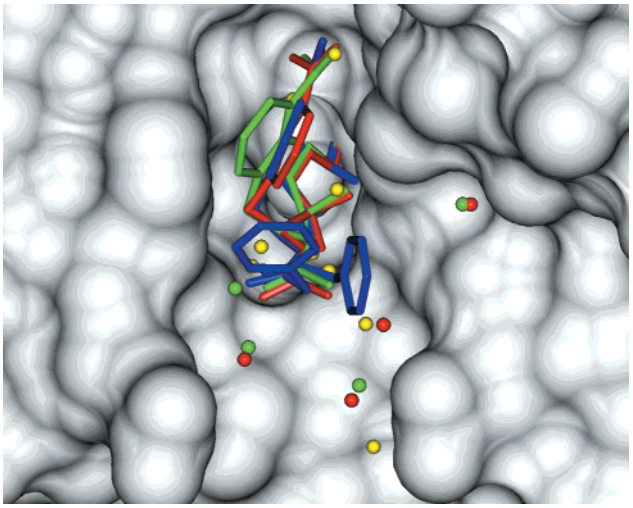

FIGURE 5: Overlap of boronate inhibitors **1** (blue), **2** (green), and **3** (red) bound to TEM-1 β-lactamase. Select ordered water molecules observed in complexes **2** and **3** and missing in complex **1** are also shown, illustrating the role of the hydrophobic phenylacetamido group of compound **1** in displacing ordered solvent from the active site. Waters observed in the structure of the native TEM-1 enzyme are also shown (yellow), illustrating the entropically favorable displacement of ordered water by the inhibitor as it binds to the active site.

TEM-1 (yellow spheres) and the TEM-1 inhibitor complexes. Clearly, compounds **2** and **3** retain several conserved ordered water molecules, whereas in compound **1**, at least three more of the ordered native water molecules have been displaced by the observed conformations of the phenylacetamido side group in addition to the oxyanion hole and deacylating water. In the structure of the acyl-enzyme intermediate of penicillin G with a mutant TEM-1 (*19*), the phenyl side group of PenG performs a similar function, displacing water and forming favorable van der Waals interactions with the relatively nonpolar atoms of Gly238 in the enzyme.

Structural Basis for Increased Affinity. Both designed inhibitors have greatly increased affinity for TEM-1 β-lactamase; there is a 19-fold increase for compound **1** and an 8.5-fold increase for compound **2** relative to the originally designed *N*-acetyl derivative **3** (Figure 1). For compound **2**, the increased affinity appears to be due primarily to increased hydrogen bonding interactions allowed by the addition of the hydroxyl group OH3. This group forms strong hydrogen bonds to three atoms (see Table 2), causing the phenylacetyl ring to which it is attached to rotate 25.6° relative to compounds **1** and **3**. This rotation also brings the phenylacetyl moiety closer to Tyr105, allowing for stronger van der Waals interactions between the two and causing a close contact between OH3 of the inhibitor and Oγ of the Ser 70. For compound **1**, the addition of the phenylacetamido ring, analogous to the phenyl ring in penicillin G, displaces multiple ordered water molecules and has van der Waals contacts with the relatively nonpolar face of residues Gly238 and Ala237. The displacement of these ordered water molecules is entropically favorable.

Future Directions. The addition of the hydroxyl group in compound **2** and the addition of the phenyl ring in compound **1** both cause increased affinity for the inhibitor to TEM-1. These two groups are separated in space and interact with different residues in the protein. Thus, it is highly likely that an additive approach to these modifications would further improve binding efficacy. A further substitution of the phenyl moiety could also be envisaged which interferes with the second binding conformation for the phenylacetamido side group, forcing it to adopt the single conformation analogous to that in PenG. In addition, there are several possible sites for polar or charged interactions in the region containing Glu166, Asn170, and Glu104, the region occupied by the side group phenylacetamido ring in compound **1**. With careful analysis, it should be possible to design appropriate polar or charged substituents onto the side group of the inhibitor which interact favorably with these side chains and thus further increase binding affinity and solubility of the transition state analogue compounds.

REFERENCES

1. Abraham, E. P., and Chain, E. B. (1940) *Nature 146*, 837.
2. Frere, J. M. (1995) *Mol. Microbiol. 16*, 385−395.
3. Matagne, A., and Frere, J. M. (1999) *Nat. Prod. Rep. 16*, 1−19.
4. Massova, I., and Mobashery, S. (1998) *Antimicrob. Agents Chemother. 42*, 1−17.
5. Bush, K., Jacoby, G. A., and Medeiros, A. A. (1995) *Antimicrob. Agents Chemother. 39*, 1211−1233.
6. Bonomo, R. A., and Rice, L. B. (1999) *Front. Biosci. 4*, 34−41.
7. Reading, C., and Cole, M. (1977) *Antimicrob. Agents Chemother. 37*, 852−857.
8. Bush, K., Macalintal, C., Rasmussen, B. A., Lee, V. J., and Yang, Y. (1993) *Antimicrob. Agents Chemother. 37*, 851−858.
9. Pratt, R. F. (1989) *Science 246*, 917−919.
10. Pratt, R. F., and Rahil, J. (1991) *Biochem. J. 275*, 793−795.
11. Chen, C. C. H., Rahil, J., Pratt, R. F., and Herzberg, O. (1993) *J. Mol. Biol. 234*, 165−179.
12. Li, N., Rahil, J., Wright, M. E., and Pratt, R. F. (1977) *Bioorg. Med. Chem. 5*, 1783−1788.
13. Maveyraud, L., Pratt, R. F., and Samama, J. P. (1998) *Biochemistry 37*, 2622−2628.
14. Bitha, P., Li, Z., Francisco, G. D., Yang, Y., Petersen, P. J., Lenoy, E., and Lin, Y. I. (1999) *Bioorg. Med. Chem. Lett. 9*, 997−1002.
15. Richter, H. G., Angelhrn, P., Hubschwerlen, C., Kania, M., Page, M. G., Specklin J. L., and Winkler, F. K. (1996) *J. Med. Chem. 39*, 3712−3722.
16. Miyashita, K., Massova, I., Taibi, P., Mobashery, S. (1995) *J. Am. Chem. Soc. 117*, 11055.
17. Maveyraud, L., Massova, I., Birck, C., Miyashita, K., Samama, J. P., and Mobashery, S. (1996) *J. Am. Chem. Soc. 118*, 971−977.
18. Buynak, J. D., Wu, K., Bachmann, B., Khasnis, D., Hua, L., Nguyen, H. K., and Carver, C. L. (1995) *J. Med. Chem. 38*, 1022−1034.
19. Strynadka, N. C. J., Adachi, H., Jensen, S. E., Johns, K., Sielecki, A., Betzel, C., Sutoh, K., and James, M. N. G. (1992) *Nature 359*, 700−705.
20. Baldwin, J. E., Claridge, T. D. W., Derome, A. E., Smith, B. D., Twyman, M., and Waley, S. G. *J.* (1991) *Chem. Soc. Chem. Commun*. 573−574.
21. Weston, G. S., Blazquez, J., Baquero, F., and Shoichet, B. K. (1998) *J. Med. Chem. 41*, 4577−4586.
22. Jones, J. B., Martin, R., and Gold, M. (1994) *Bioorg. Med. Chem. Lett. 4*, 1229.
23. Martin, R., and Jones, J. B. (1995) *Tetrahedron Lett. 36*, 8399−8402.
24. Strynadka, N. C. J., Martin, R., Gold, M., Jensen, S. E., and Jones, J. B. (1996) *Nat. Struct. Biol. 3*, 688−695.
25. Escobar, W. A., Tan, A. K., and Fink, A. L. (1991) *Biochemistry 30*, 10783−10787.
26. Oefner, C., D'Arcy, A., Daly, J. J., Gubernator, K., Charnas, R. L., Heinze, I., Hubschwerlen, C., and Winkler, F. K. (1990) *Nature 343*, 284−288.

27. Taibi, P., and Mobashery, S. J. (1995) *J. Am. Chem. Soc. 117*, 7600−7605.
28. Vijayakumar, S., Ravishanker, G., Pratt, R. F., and Beveridge, D. L. (1995) *J. Am. Chem. Soc. 117*, 1722−1730.
29. Miyashita, K., Massova, I., Taibi, P., and Mobashery, S. (1995) *J. Am. Chem. Soc. 117*, 11055−11059.
30. Jelsch, C., Mourey, L., Mason, J. M., and Samama, J. P. (1993) *Proteins: Struct., Funct., Genet.*, 364−383.
31. Herzberg, O., and Moult, J. (1987) *Science 236*, 694−701.
32. Knox, J. R., and Moews, P. C. (1991) *J. Mol. Biol. 220*, 156−171.
33. Swaren, P., Maveyraud, L., Raquet, X., Cabantous, S., Duez, C., Pedelacq, J. D., Mariotte-Boyer, S., Mourey, L., Labia, R., Nicolas-Chanoine, M. H., Nordmann, P., Frere, J.-M., and Samama, J. P. (1998) *J. Biol. Chem. 273*, 26714−26721.
34. Kuzin, A. P., Nukaga, M., Nukaga, Y., Hujer, A., Bonomon, R. A., and Knox, J. R. (1999) *Biochemistry 38*, 5720−5727.
35. Hurd, C. D., and Prapas, A. G. (1959) *J. Org. Chem. 24*, 388−392.
36. Doran, J. L., Leskiw, B. K., Aippersbach, S., and Jensen, S. E. (1990) *J. Bacteriol. 172*, 4909−4918.
37. Waley, S. G. (1982) *Biochem. J. 205*, 631−633.
38. Waley, S. G., and Cartwright, S. J. (1984) *Biochem. J. 221*, 505−512.
39. Lowe, G., Crompton, I. E., Cuthbert, B. K., and Waley, S. G. (1988) *Biochem. J. 251*, 453−459.
40. Otwinowski, A. (1993) in *DENZO 1993* (Sawyer, L., Isaacs, N., and Bailey, S., Eds.) pp 56−62, SERC Daresbury Laboratory, Warrington, U.K.
41. Research Collaboratory for Structural Bioinformatics (http:/www.rcsb.org/pdb/).
42. Matteson, D. S. (1989) *Chem. Rev. 89*, 1535−1551.
43. Kettner, C. A., and Shenri, A. B. (1984) *J. Biol. Chem. 259*, 15106−15110.
44. Pudleiner, H., and Laatsch, H. (1989) *Synthesis*, 286−287.
45. Huston, R. C., and Neeley, A. H. (1935) *J. Am. Chem. Soc. 57*, 2176−2178.
46. Solladie, G., et al. (1990) *Tetrahedron Asymm. 1*, 187−198.
47. Micheli, R. A., Hajos, Z. G., Cohen, N., Parrish, D. R., Portland, L. A., Samama, W., Scott, M. A., and Wehrli, P. A. (1975) *J. Org. Chem. 40*, 675−682.
48. Meyers, A. I., Temple, D. L., Haidukewych, D., and Mihelich, E. D. (1974) *J. Org. Chem. 39*, 2787−2793.
49. Nyzam, V., Belend, C., and Villieras, J. (1993) *Tetrahedron Lett. 34*, 6899−6902.
50. Keana, J. F., and Cai, S. X. (1991) *Bioconjugate Chem. 2*, 317−322.
51. Matteson, D. S., Michnick, T. J., Willet, R. D., and Patterson, C. D. (1989) *Organometallics 8*, 726−729.
52. Mobashery, S., Bulychev, A., Massova, I., and Lerner, S. A. (1995) *J. Am. Chem. Soc. 117*, 4797−4801.
53. Coleman, K., Griffin, D. R., Page, J. W. J., and Upshon, P. A. (1989) *Antimicrob. Agents Chemother. 33*, 1580−1587.
54. Knowles, J. R., and Charnas, R. L. (1981) *Biochemistry 20*, 2732−2737.
55. Pratt, R. F. (1989) *Science 246*, 917−919.
56. Pratt, R. F., and Rahil, J. (1991) *Biochem. J. 275*, 793−795.
57. Page, M. I., Laws, A. P., Slater, M. J., and Stone, J. R. (1995) *Pure Appl. Chem. 67*, 711.
58. Pratt, R. F., and Rahil, J. (1993) *Biochemistry 32*, 10763−10772.
59. Page, M. I., Laws, A. P., and Slater, M. J. (1993) *Bioorg. Med. Chem. Lett. 11*, 2317−2322.
60. Tronrud, D. E. (1992) *Acta Crystallogr. A48*, 912−916.
61. Kissinger, C. R., Gehlhaar, D. K., and Fogel, D. B. (1999) *Acta Crystallogr. D55(Pt 2)*, 484−491.

BI992505B